Frontiers of Physics
https://doi.org/10.1007/s11467-020-1000-6
Front. Phys.
16(2), 23501 (2021)

RESEARCH ARTICLE

Dense skyrmion crystal stabilized through interfacial exchange coupling: Role of in-plane anisotropy

Ming-Xiu Sui[1], Zi-Bo Zhang[1], Xiao-Dan Chi[1], Jia-Yu Zhang[1], Yong Hu[1,2,†]

[1] *Department of Physics, College of Sciences, Northeastern University, Shenyang 110819, China*
[2] *State Key Laboratory of Rolling and Automation, Northeastern University, Shenyang 110819, China*
Corresponding author. E-mail: †huyong@mail.neu.edu.cn
Received June 29, 2020; accepted September 9, 2020

A Monte Carlo simulated-annealing algorithm was used to study the magnetic state in an in-plane helimagnet layer on triangular lattice that exchange couples to an underlayer with strong out-of-plane anisotropy. In the single helimagnet layer with in-plane anisotropy (K), the formation of labyrinth-like domains with local spin spirals, instead of parallel stripes, is favored, and these domains rapidly transform into dense skyrmion crystals with increasing interfacial exchange coupling (J'), equivalent to a virtual magnetic field, and finally evolve to an out-of-plane uniform state at large enough J'. Moreover, with increasing K, the skyrmion crystal state can vary from regular 6-nearest-neighboring circular skyrmion arrangement to irregular squeezed skyrmions with less than 6 nearest neighbors when the in-plane anisotropy energy is higher than the interfacial exchange energy as the skyrmion number is maximized. Finally, we demonstrated that the antiferromagnetic underlayer cannot induce skyrmions while the chirality inversion can be achieved on top of an out-of-plane magnetization underlayer with 180° domain walls, supporting the experimental findings in FeGe thin film. This compelling advantage offers a fertile playground for exploring emergent phenomena that arise from interfacing magnetic skyrmions with additional functionalities.

Keywords skyrmion, thin-film, interfacial exchange coupling, in-plane anisotropy, Monte Carlo simulation

1 Introduction

Magnetic skyrmions are nanoscale swirling spin textures exhibiting a nontrivial real-space topology, which confer on them quasiparticlelike properties that, combined with their ability to be moved by electrical current, make them promising candidates for storage and manipulation of information [1, 2]. Generally, skyrmions are explained by the existence of Dzyaloshinskii–Moriya interaction (DMI) [3, 4], as it favors magnetic spins on neighboring atomic sites to be aligned orthogonally with a fixed chirality [5]. This coupling originates from the combination of low structure symmetry and large spin–orbit coupling, and thus it may exist either in bulk materials lacking space inversion symmetry [4], or at interfaces between a magnetic film and a high spin–orbit coupling adjacent layer [6, 7]. By recalling that the DMI energy is $-\boldsymbol{D}_{ij}\cdot(\boldsymbol{S}_i\times\boldsymbol{S}_j)$, where $\boldsymbol{D}_{ij}$ is the DMI vector, and $\boldsymbol{S}_i$ and $\boldsymbol{S}_j$ are spins at two neighboring sites i and j, in bulk materials $\boldsymbol{D}_{ij}$ is parallel to the distance vector $\boldsymbol{r}_{ij}$ between sites, in contrast to the thin-film systems, where $\boldsymbol{D}_{ij}$ is usually perpendicular to $\boldsymbol{r}_{ij}$ [4, 8]. As a result, different orientations of $\boldsymbol{D}_{ij}$ cause Bloch- and Néel-type homochiral skyrmions in bulk and thin-film systems, respectively, categorized by distinct non-trivial topological properties such as spiral and hedgehog textures. The chirality of skyrmions can be analyzed more quantitatively by measuring statistical distribution of magnetization directions as a function of location with respect to skyrmion centers [9–11]. Taking micromagnetic view of DMI, which is valid in the limit of slowly varying magnetic textures, skyrmions can be identified by a topological charge, or called $\mathbb{S}^2$ winding number $\tau=\pm1$ [2, 12], where

$$\tau=\frac{1}{4\pi}\int_{\mathbb{R}^2}\boldsymbol{S}\cdot(\partial_x\boldsymbol{S}\times\partial_y\boldsymbol{S})\,\mathrm{d}\boldsymbol{r}. \tag{1}$$

Actually, the DMI, coexisting with the ferromagnetic exchange $\boldsymbol{S}_i\cdot\boldsymbol{S}_j$, only favors a spin-spiral phase, characterized by a single wave number $\boldsymbol{q}$ [13]. In order to trigger and stabilize skyrmions, one approach is to add the Zeeman energy by applying an external magnetic field. The spin-spiral competes with ferromagnetism, breaking the symmetry of up and down domains in the spin-spiral configuration, and thus an ordered skyrmion-crystal (SkC) or a partially disordered nucleated skyrmion-gas phase, with

*This article can also be found at http://journal.hep.com.cn/fop/EN/10.1007/s11467-020-1000-6.

$3\boldsymbol{q}$ values, emerges at intermediate field strengths. To be more compatible with technological developments, effective and well controlled writing and reading processes, i.e., the creation and manipulation of skyrmions, in thin films at room temperature and in zero field will have to be implemented. Experimentally, one has found that geometrical confinement and interfacial exchange coupling generated by additional magnetic elements can replace the external magnetic field to stabilize skyrmions [14–18]. Sun *et al.* [15] proposed a method to generate SkC phases artificially through putting the ordered arrays of nano-sized magnetic Co disks on top of CoPt film with perpendicular anisotropy. Using the similar method, Gilbert *et al.* [16] put Co nanodots on top of Co/Pd film and realized the ground-state artificial SkC phases at room temperature. They both presented that the artificially constructed SkC phases were controlled by the interfacial exchange coupling and thus did not tend to exist in limited temperature-magnetic field parameter space. Chen *et al.* [17] and Nandy *et al.* [18] found that the similar phase transition from spin-spiral, to SkC, and to the saturated state can also happen with increasing interfacial exchange coupling, while the role of interfacial exchange coupling played on the skyrmion phases at small/large in-plane magnetic anisotropies still need to be addressed.

On the other hand, in helimagnet thin-film materials, it has been found that the uniaxial magnetocrystalline anisotropy along with the out-of-plane applied field can favor to stabilize SkC state [19, 20]. When the spins experience in-plane anisotropy, the SkC state is also observed while evolve in different manners [21, 22]. Lin *et al.* [21] and Vousden *et al.* [22] both presented that the size of skyrmion increases with increasing in-plane magnetocrystalline anisotropy, and Lin *et al.* [21] further reported that the magnetic state evolves into a regime where the nearest-neighbor skyrmions start overlapping with each other and found a transition of SkC from a triangular to a square lattice with increasing in-plane anisotropy. The in-plane anisotropy in helimagnet thin films can provide a contribution to Hall resistivity [23, 24], which may be interpreted as topological Hall effect, arising through real space Berry phase effects [25]. The demonstration of relationship between SkC and in-plane anisotropy encourages research into a broader range of materials for skyrmion physics and spintronic applications [26]. In this work, we numerically study the zero-field magnetic phase transition of a helimagnet thin film with in-plane anisotropy on triangular lattice exchange coupled to an underlayer through stacked or closed-packed structure. A systematic investigation on SkC state and its evolution as a function of interfacial exchange coupling and in-plane anisotropy is presented.

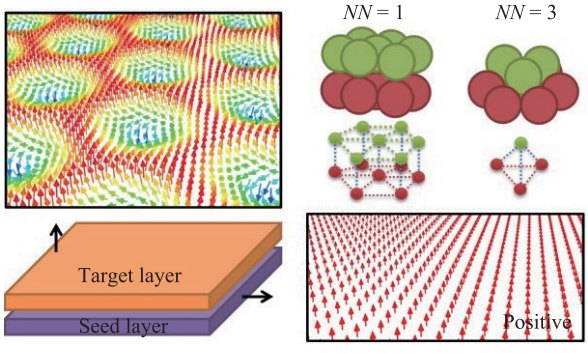

Fig. 1 Structure of the bilayer where a helimagnet target layer is on top of an out-of-plane magnetization seed layer. The green and red spheres represent atoms in the target and seed layers and indicate two crystal structures: interfacial stacked and closed-packed structures, labeled by the nearest-neighboring (NN) interfacial spin number.

2 Model

In the simulation, two monolayers are used to stand for the target and seed layers, and each layer consists of $N = 10\,000$ spins which are placed on the nodes of triangular lattice with in-plane periodic boundary conditions. In reality, the atoms in the target layer placed on the interstitial space of the three atoms of the seed layer, leading to three nearest-neighboring (NN) interfacial spin number, i.e., $NN = 3$, are the common way of the atom stacking along (111) direction for the target layer with bulk DMI, which requires the inversion symmetry breaking, e.g., B20 structure. In this work, the role of interfacial exchange coupling played on the creation and annihilation of skyrmions was focused on to be demonstrated. Hence, the other NN interfacial spin number ($NN = 1$) is set, where the atoms in the target layer occupy the top-sites of the atoms of the seed layer, for presentation of a quantitative interpretation, as shown in Fig. 1.

The Hamiltonian in the absence of a magnetic field can read as

$$\begin{aligned}\mathcal{H} = &- J \sum_{\langle i,j\in \text{ Target Layer}\rangle} \boldsymbol{S}_i \cdot \boldsymbol{S}_j \\ &- D \sum_{\langle i,j\in \text{ Target Layer}\rangle} \boldsymbol{r}_{ij} \cdot (\boldsymbol{S}_i \times \boldsymbol{S}_j) \\ &- K \sum_{i\in \text{ Target Layer}} (\boldsymbol{S}_i \cdot \hat{e}_i)^2 \\ &- J' \sum_{\langle i\in \text{ Target Layer},\, k\in \text{ Seed Layer}\rangle} \boldsymbol{S}_i \cdot \boldsymbol{S}_k, \end{aligned} \tag{2}$$

where $\boldsymbol{S}_{i(j,k)}$ is the unit vector of spin $i(j,k)$ and $\hat{e}_i$ is the unit vector of anisotropy. In Eq. (2), the energies of intralayer exchange interaction, DMI and in-plane anisotropy in the target layer and the interfacial exchange energy between target and seed layers are considered. Angular brackets indicate the summations over the NN spin pairs. In the B20-structure thin-films, such as MnSi, FeGe and insulators like Cu_2OSeO_3, the systems may break surface-inversion in addition to bulk inversion. Rowland *et*

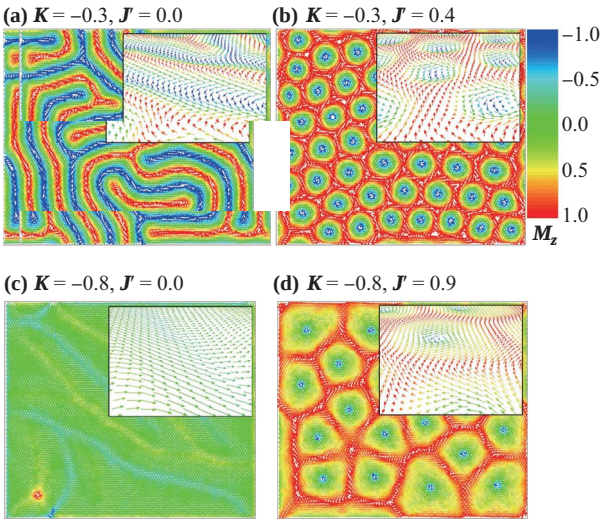

Fig. 2 Spin configurations for selected K and J', where arrows represent the spin orientations and color shows the z-component of magnetization. Insets show the zoomed-in 3D view.

al. [27] have reported that the increase of interfacial DMI in the presence of the bulk DMI will greatly help stabilize skyrmion phases. Due to the DMI that exists in helimagnet target layer only, the bulk-type DMI with the $\boldsymbol{D}_{ij}$ parallel to $\boldsymbol{r}_{ij}$ is involved, identical to that used in Ref. [21] and [22]. This work focuses on the role of K and J', and for simplicity, the interfacial DMI contribution is not taken into account in Eq. (2). In other words, the seed magnetic layer with perpendicular anisotropy only provides an exchange field, analogous to a virtual magnetic field, applied on the upper target chiral magnetic layer, hence it is different from the case of the DMI induced at interfaces [6, 7], where a Néel-typed skyrmion is favored. Moreover, $\hat{e}_i = \hat{z}$ and $K < 0$, resulting in the spins in the target layer that favor to lie in the film plane (xy-plane) to minimize the anisotropy energy. Finally, the S_k in the seed layer is set to be $\pm\hat{z}$ to form different out-of-plane magnetic orderings. All of the magnetic parameters used are reduced to be dimensionless by the intralayer exchange coupling constant J. Hence, $J = 1$ and $D/J = 0.6$ are fixed, while $J'/J = 0$–1.3 and $K/J = -1.1$–0 are adjustable to study their roles played on establishing the SkC configurations. Finally, the model established mimics the ultrathin films with only one or several monolayers, where the dipolar coupling becomes local in the zero-thickness limit [28], similar to the one-monolayer film model adopted by Cortés-Ortuño *et al.* [14]. On the other hand, in the 2D thin-film structures, the role of dipolar interactions played has proven to tend to make the spins head-to-tail align in the film plane [29], which has also been realized by in-plane magnetic anisotropy and ferromagnetic exchange coupling. In view of Jiang *et al.*'s findings [1, 30], the dipolar interactions associated with DMI favor to form big skyrmions with diameters even in the micrometer range. Therefore, the dipolar interactions only quantitatively, other than qualitatively, change the J'–K range where skyrmions appear and affect the skyrmion size, and thus are safely ignored in Eq. (2). The Monte Carlo simulation starts from a zero-field-cooled process performed on the system with magnetically disordered state. The initial high temperature is set as $T_0 = 10\ J/k_B$, where k_B is Boltzmann constant, and the next temperature is 5% smaller than the previous one. Hence the final low temperature is calculated by $T = 0.95^{136}T_0$. At each temperature, 20000 Monte Carlo steps were performed based on the simulated-annealing algorithm [31]. The final observables were calculated from thermalized spin configurations and Monte Carlo averaged with 30 different realizations.

3 Results and discussion

For the single helimagnet layer, i.e., $J' = 0$ meanwhile with not too large K, e.g., $K/J = -0.3$, the labyrinthian belts with equal width is formed, and the spin orientations in the adjacent belts are opposite. After cooling, the competition between DMI and intralayer exchange interaction favors the spin-spiral state, nevertheless, the in-plane anisotropy at finite temperature results in no existence of favored spin-spiral directions in the film plane and thus the formation of labyrinth domains. However, if K is large enough ($K/J = -0.8$), the spin-spiral state is broken and the spins are lying in the film plane to minimize the anisotropy energy, and the intralayer exchange interaction and the DMI contribute to the formation of in-plane random domains. For the helimagnet layer with $K/J = -0.3$ coupled to a ferromagnetic underlayer with the positive z-direction magnetization via $J'/J = 0.4$, a dense and regular SkC state is observed, where each circular skyrmion with the same size is encircled by six nearest neighbors. As mentioned previous, if $J' = 0$, the DMI and ferromagnetic coupling in the chiral magnetic film only favor to form spin-spiral states and at finite temperatures, the parallel spin-spiral stripes are replaced by labyrinth states. As the interfacial exchange coupling is introduced, the equidistant distribution of the positive and negative out-of-plane components of magnetization is broken. The positive out-of-plane magnetization in the seed layer via ferromagnetic interfacial exchange coupling widens the positive component meanwhile squeezes the negative component. The bulk DMI in the spin-spiral state causes the spins to rotate from positive to negative out-of-plane direction through Bloch-type domain walls, which are also stabilized by in-plane magnetic anisotropy. When the balance between up and down spins is broken by J', the down spins are protected from more up spins by the spins circling around the down spins, and thus the skyrmions form. It is remarkable that the skyrmions with a center of negative out-of-plane magnetization involved in the positive out-of-plane magnetization exhibit Bloch-

type with homochirality ($\tau = -1$) due to the existence of bulk DMI. In other words, the interfacial exchange coupling controls the out-of-plane magnetization, while the DMI determines the in-plane one. Furthermore, the control of chirality can be realized by adjusting the sign of out-of-plane magnetization in the seed layer, which will be presented and discussed later. At large $K/J = -0.8$ and $J'/J = 0.9$, the skyrmions expand and deform due to their squeezing with each other, and for each skyrmion, its NN number may be less than six. In other words, the SkC state remains while becomes irregular. For distinguishing them, the regular SkC state is called the SkC-I type, while the irregular SkC state called the SkC-II type.

Magnetic skyrmion is a promising block for building future spintronic applications, as it can be employed as a non-volatile information carrier in magnetic media. Hence, controllable and reliable creation and annihilation of skyrmions are prerequisites for any skyrmion-based information storage applications. It is a vital task to demonstrate K and J' ranges to write and delete skyrmions. Based on the calculated skyrmion charge density ($w = \sum\tau/N$), the J'–K phase diagrams for the bilayer established by stacked ($NN = 1$) and closed-packed ($NN = 3$) structures are obtained in Fig. 3. For $NN = 1$, at $J' = 0$ and $|K/J| < 0.6$, the labyrinth domain is the ground state in helimagnet layer. With increasing J', the skyrmions appear even at $J'/J = 0.1$, mixed with the stripe domains. From $J'/J = 0.2$, the dense and regular SkC-I typed domain is formed, and w increases initially and then decreases with J', associated with the skyrmions that shrink firstly and then expand. Finally, the SkC state evolves to the out-of-plane uniform state at critical J' value, which is proportional to K. Interestingly, for $|K/J|$ higher than 0.6, the SkC-II typed domain with reduced w is observed at appropriate J', partially similar to Lin *et al.*'s calculated results [21]. The large K encourages the skyrmion growth, resulting in the overlap between adjacent skyrmions. Differently, at finite temperature after cooling, the total energy can be minimized in the system where there are skyrmions with different sizes and nearest neighbors, analogue to the spin assembly in a spin glass [32, 33]. With further increasing J' at K/J close to -0.6, the out-of-plane uniform state is also obtained, while at large K and small J', i.e., on the left and lower corner of phase diagram in Figs. 3(a, c), the in-plane random domains as seen in Fig. 2(c) are favored. On the left and upper corner where K and J' are both large, the canted domains have to be favored to minimize the interfacial exchange and in-plane anisotropy energies simultaneously.

As compared to the results obtained for $NN = 1$, different phases can also be found for $NN = 3$ and the highest skyrmion charge density remains same, however, the magnetic phase transition occurs from the labyrinth, to the SkC-I, and to the out-of-plane uniform state in a narrower J' range from $J' = 0$. For external stimuli such as magnetic field applied perpendicular to the magnetic film with DMI, a small magnetic field is required for the formation of skyrmions, while a large magnetic field could lead to collapse and annihilation of skyrmions, meanwhile, the skyrmion size commonly decreases monotonically with increasing magnetic field [34–36], arising from the external magnetic field that interplays with other energetic contributions, e.g., DMI, magnetic anisotropy, demagnetization energy and exchange interaction. In this work, J' is equivalent to a virtual out-of-plane magnetic field, while also depends on the interfacial crystal structure, i.e., interfacial coordinate number (NN value). When we com-

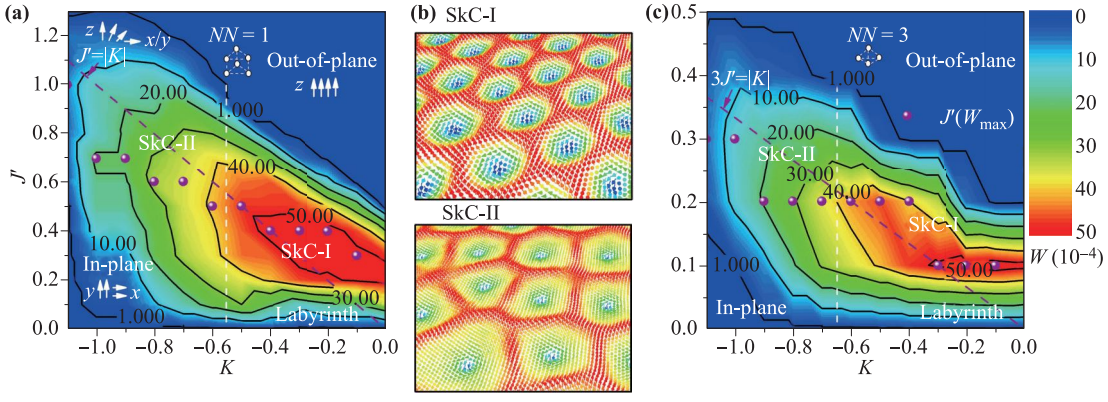

Fig. 3 Phase diagram with respect to J' and K for **(a)** the interfacial stacked ($NN = 1$) and **(c)** closed-packed ($NN = 3$) structures, schematically shown by white dots, where color is the skyrmion charge density (w) result with contour lines, and different phases with their characteristic configurations for large K and/or J', schematically shown by white arrows, are also indicated. Purple solid spheres give the J' as a function of K where w reaches to the maximum at a given K and purple dashed lines show the interfacial exchange energy that is equal to the anisotropy energy. White vertical dashed lines are used to separate different skyrmion-crystal (SkC) types. **(b)** The representative 3D skyrmion configurations of SkC-I and SkC-II typed states.

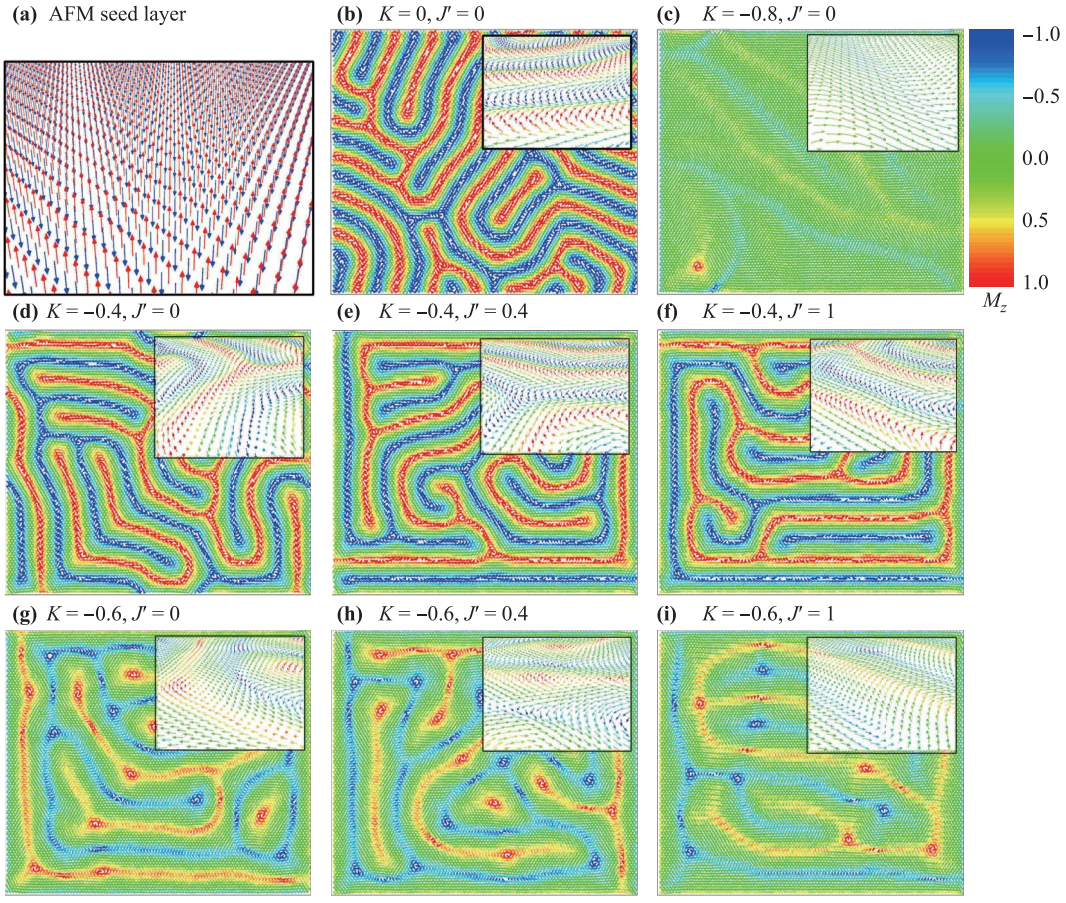

Fig. 4 **(a)** Antiferromagnetic configuration of the seed layer. **(b–i)** Spin configurations of the helimagnet layer coupled to an antiferromagnetic underlayer for selected K and J', where arrows represent the spin orientations and color shows the z-component of magnetization. Insets show the zoomed-in 3D view.

pared the K and J' values to obtain the most skyrmions with those that yield the same interfacial exchange and in-plane anisotropy energies, i.e., $J' = |K|$ for $NN = 1$ or $3J' = |K|$ for $NN = 3$, it is found that the SkC-I state is stabilized so long as w is maximized for the J' energy higher than the K energy, or the SkC-II state is preferred. In other words, the SkC type reflects the energy level of K and J'. Significantly, more coordinate number at interface can proportionally reduce J', implying that the J' range of SkC can be adjustable through properly matching dissimilar materials besides manipulating spacer thickness experimentally [17].

In Chen *et al.*'s experiment [17], the Cu/Ni/Cu(001) trilayer was used to generate a stable out-of-plane magnetization pointing to the positive z-direction, and in Nandy *et al.*'s theoretical study [18] also assumed an uniform ferromagnetic underlayer as the ferromagnetic seed layer similar to that shown in Fig. 1. If the underlayer is replaced by an antiferromagnetic layer or a magnetic layer with a 180° domain wall with the spins keeping along the z axis, what happens for the magnetic state in the upper helimagnet layer with K and J'? For the antiferromagnetic underlayer, the labyrinth domain appears at small K, while the in-plane random domain is stabilized at large K, and no skyrmions or SkC states can be observed in the whole studied J' range. As shown in Figs. 4(b, d–f), the stripe width is roughly independent of J', although different patterns are obtained, indicating that the labyrinth domain with alternate opposite magnetic states completely arises from the interplay between DMI and intralayer exchange interaction in the helimagnet layer. In other words, J' does not take effect due to the interfacial exchange coupling imposed by the neighboring spin pair in the underlayer that cancels out. Moreover, at large K, the in-plane anisotropy is so predominant that the stripe domains are smeared out and the resultant in-plane random domains are formed, also regardless of J', as shown in Figs. 4(c, g–i).

Further, we conceive a magnetic underlayer with coexisting positive and negative magnetization with respect to the positive z-direction, and thus there is 180° domain wall [seen in the inset of Fig. 5(b)]. For $K/J = -0.3$, even at small J'/J $(= 0.1)$, the line domains with the spins pointing along the y-axis exist on top of domain wall to

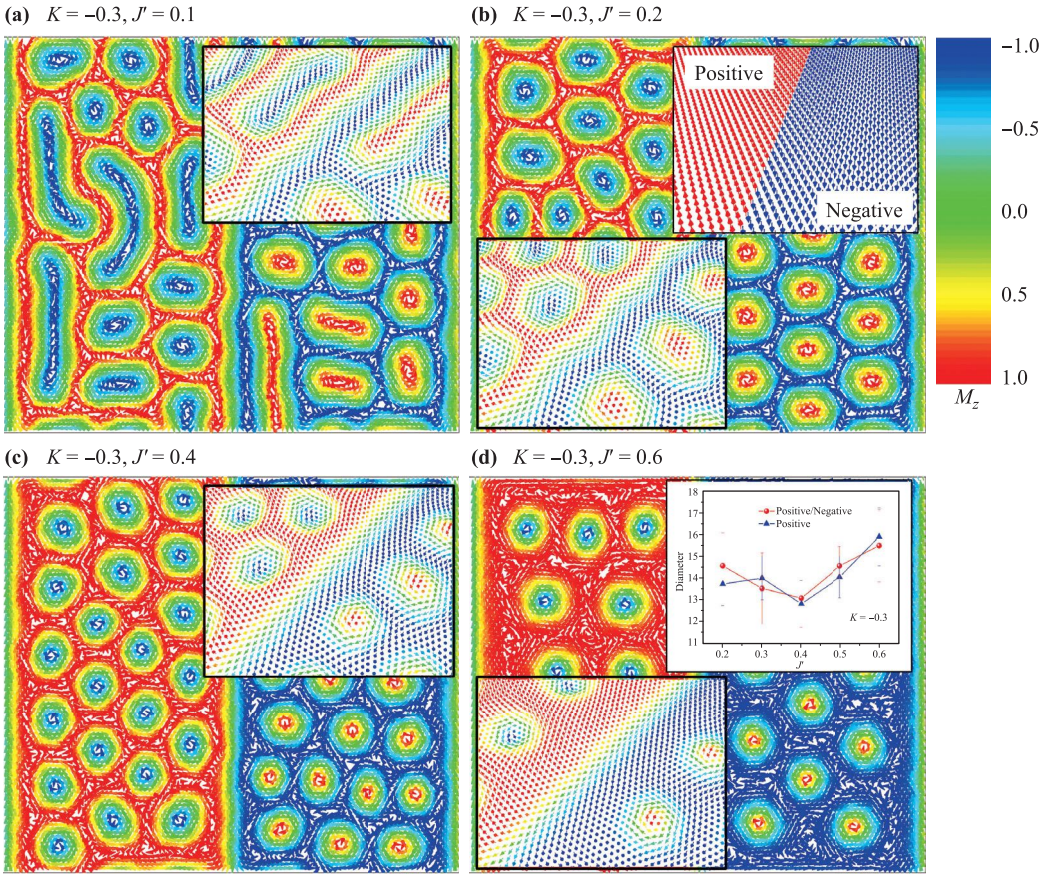

Fig. 5 Spin configurations of the helimagnet layer coupled to an out-of-plane magnetization underlayer with the 180° domain wall for selected K and J', where arrows represent the spin orientations and color shows the z-component of magnetization. Inset in **(b)** gives the spin configuration of seed layer and inset in **(d)** shows the skyrmion diameter as a function of J' at $K/J = -0.3$ for the seed layer with the positive/negative and positive z-direction magnetization, where errors are determined by calculating all of the skyrmion diameters in the SkC-I state. Insets also show the zoomed-in 3D view.

minimize the J' energy due to the opposite spin arrangement on the both sides of the domain wall, similar to Koon's orthogonal interface model presented in ferromagnet/antiferromagnet thin-film [37]. On top of the uniform magnetization area, the mixed domains with skyrmions and stripes are preferred, and interestingly, the stripe domains favor to appear parallel to the domain wall, similar to the stripe domains in thin helimagnet nanodisk [38]. With increasing J'/J from 0.2 to 0.6, the SkC-I typed state is formed, while no skyrmions appear on top of the domain wall. In FeGe nanostripes, Du *et al.* [39] found that the skyrmions were created from helices with a distorted edge state and move collectively into the interior of the stripe with increasing magnetic field. In this work, the underlayer domain wall fixes the upper spins parallel to it, similar to the edge effect, resulting in the coexistence of the SkC state on top of the positive and negative magnetization with the opposite chirality ($\tau = -1$ and 1). However, differing from the experimental findings by Du *et al.* [39], the correlation between skyrmion creation and domain wall is weak in this work, probably due to lacking of a field in the chiral magnetic film plane applied perpendicular to the domain wall. Furthermore, in helimagnet FeGe thin film, Yu *et al.* [40] presented that a chirality inversion was found around the grain boundary between (110) and (001) planes. Considering the invariance of sign of spin–orbit interaction within FeGe, the observed reversal of the SkC spin chirality is ascribed to the inversion of lattice chirality (handedness) of B20 structure across this boundary. It indicates that the chirality inversion exists naturally in helimagnet thin-film, while in this work an artificial chirality inversion around the 180° domain wall is achieved. In other words, by choosing proper magnetic parameters and attaching an underlayer with well-designed magnetic domain pattern, the precise writing of skyrmions with organized chirality ordering is possible. On the other hand, with increasing J', the skyrmion diameter initially decreases, reaches to the minimum at $J'/J = 0.4$, and then increases for larger J'. On the contrary, it is well-known that the skyrmion diameter monotonically decreases with increasing magnetic field [34–36], which is acceptable that the magnetic field

drives the spins at the perimeter of skyrmions to align with its direction and thus the skyrmions shrink continuously. In the present work, the skyrmions are stabilized by the lower magnetic film with perpendicular magnetic anisotropy via J'. Comparing with the results shown in Fig. 3(a) and Fig. 5, the smallest skyrmions correspond to the largest skyrmion charge density at $K/J = -0.3$ and $J'/J = 0.4$, where the skyrmions are densely arranged and squeeze by each other. With further increasing J', some skyrmions collapse and annihilate, which leaves additional space between adjacent skyrmions. Thus, associated with the reduced skyrmion charge density, the skyrmions are expanded spontaneously to cancel out the residual energy due to disappearance of high squeezing between adjacent skyrmions at large J'. Note that no thickness of domain wall is considered, since the domain wall cannot contribute to the SkC state and the domain wall thickness only widens the isolation belt of skyrmions with opposite chirality.

4 Conclusion

In conclusion, Monte Carlo simulation was performed on a helimagnet layer model coupled to an underlayer with strong out-of-plane anisotropy, to study the magnetic state stabilized by J' and the role played by K. At low temperature after zero-field-cooling, the labyrinth domain is the ground state in single helimagnet layer. With increasing J', the dense SkC state may be obtained and categorized as regular and irregular arrangements, depending on K. The skyrmion diameter with such J' internal stimuli decreases initially and then increases. We also identified that the transition between the two typed SkC states occurs when the interfacial exchange energy is equal to the in-plane anisotropy energy, and significantly, the interfacial exchange coupling as a virtual magnetic field can be also highly reduced by increasing the interfacial coordinate number. Moreover, the local ferromagnetic domains in the positive and negative z-direction with a 180° domain wall induced a chirality inversion of skyrmions, which may be used to record "1" and "0" information at will. This work not only fertilizes the fundamental understanding of skyrmions, but also opens a new avenue for envisaging the devices with desired SkC ground-states for practical applications.

Acknowledgements The authors express their thanks to Dr. Gong Chen helping with this work. This work was financially supported by the National Natural Science Foundation of China (No. 11774045), the Joint Research Fund Liaoning-Shenyang National Laboratory for Materials Science (No. 20180510008), and the Fundamental Research Funds for Central Universities (No. N182410008-1).

References

1. A. Fert, N. Reyren, and V. Cros, Magnetic skyrmions: Advances in physics and potential applications, *Nat. Rev. Mater.* 2(7), 17031 (2017)
2. X. Zhang, Y. Zhou, K. Mee Song, T. E. Park, J. Xia, M. Ezawa, X. Liu, W. Zhao, G. Zhao, and S. Woo, Skyrmion-electronics: writing, deleting, reading and processing magnetic skyrmions toward spintronic applications, *J. Phys.: Condens. Matter* 32(14), 143001 (2020)
3. I. Dzyaloshinsky, A thermodynamic theory of "weak" ferromagnetism of antiferromagnetics, *J. Phys. Chem. Solids* 4(4), 241 (1958)
4. T. Moriya, Anisotropic superexchange interaction and weak ferromagnetism, *Phys. Rev.* 120(1), 91 (1960)
5. A. N. Bogdanov and U. K. Rößler, Chiral symmetry breaking in magnetic thin films and multilayers, *Phys. Rev. Lett.* 87(3), 037203 (2001)
6. A. Fert and P. M. Levy, Role of anisotropic exchange interactions in determining the properties of spin-glasses, *Phys. Rev. Lett.* 44(23), 1538 (1980)
7. A. Fert, Magnetic and transport properties of metallic multilayers, *Mater. Sci. Forum* 59–60, 439 (1991)
8. A. Fert, V. Cros, and J. Sampaio, Skyrmions on the track, *Nat. Nanotechnol.* 8(3), 152 (2013)
9. G. Chen, T. Ma, A. T. N'Diaye, H. Kwon, C. Won, Y. Wu, and A. K. Schmid, Tailoring the chirality of magnetic domain walls by interface engineering, *Nat. Commun.* 4(1), 2671 (2013)
10. G. Chen, A. T. N'Diaye, Y. Wu, and A. K. Schmid, Ternary superlattice boosting interface-stabilized magnetic chirality, *Appl. Phys. Lett.* 106(6), 062402 (2015)
11. G. Chen, A. T. N'Diaye, S. P. Kang, H. Y. Kwon, C. Won, Y. Wu, Z. Q. Qiu, and A. K. Schmid, Unlocking Bloch-type chirality in ultrathin magnets through uniaxial strain, *Nat. Commun.* 6(1), 6598 (2015)
12. M. Hoffmann, B. Zimmermann, G. P. Müller, D. Schürhoff, N. S. Kiselev, C. Melcher, and S. Blügel, Antiskyrmions stabilized at interfaces by anisotropic Dzyaloshinskii–Moriya interactions, *Nat. Commun.* 8(1), 308 (2017)
13. S. Banerjee, O. Erten, and M. Randeria, Ferromagnetic exchange, spin–orbit coupling and spiral magnetism at the $LaAlO_3/SrTiOO_3$ interface, *Nat. Phys.* 9(10), 626 (2013)
14. D. Cortés-Ortuño, N. Romming, M. Beg, K. von Bergmann, A. Kubetzka, O. Hovorka, H. Fangohr, and R. Wiesendanger, Nanoscale magnetic skyrmions and target states in confined geometries, *Phys. Rev. B* 99(21), 214408 (2019)
15. L. Sun, R. X. Cao, B. F. Miao, Z. Feng, B. You, D. Wu, W. Zhang, A. Hu, and H. F. Ding, Creating an artificial two-dimensional skyrmion crystal by nanopatterning, *Phys. Rev. Lett.* 110(16), 167201 (2013)

16. D. A. Gilbert, B. B. Maranville, A. L. Balk, B. J. Kirby, P. Fischer, D. T. Pierce, J. Unguris, J. A. Borchers, and K. Liu, Realization of ground-state artificial skyrmion lattices at room temperature, *Nat. Commun.* 6(1), 8462 (2015)

17. G. Chen, A. Mascaraque, A. T. N'Diaye, and A. K. Schmid, Room temperature skyrmion ground state stabilized through interlayer exchange coupling, *Appl. Phys. Lett.* 106(24), 242404 (2015)

18. A. K. Nandy, N. S. Kiselev, and S. Blügel, Interlayer exchange coupling: A general scheme turning chiral magnets into magnetic multilayers carrying atomic-scale skyrmions, *Phys. Rev. Lett.* 116(17), 177202 (2016)

19. M. N. Wilson, A. B. Butenko, A. N. Bogdanov, and T. L. Monchesky, Chiral skyrmions in cubic helimagnet films: The role of uniaxial anisotropy, *Phys. Rev. B* 89(9), 094411 (2014)

20. Y. Hu, X. Chi, X. Li, Y. Liu, and A. Du, Creation and annihilation of skyrmions in the frustrated magnets with competing exchange interactions, *Sci. Rep.* 7(1), 16079 (2017)

21. S. Z. Lin, A. Saxena, and C. D. Batista, Skyrmion fractionalization and merons in chiral magnets with easy-plane anisotropy, *Phys. Rev. B* 91(22), 224407 (2015)

22. M. Vousden, M. Albert, M. Beg, M. A. Bisotti, R. Carey, D. Chernyshenko, D. Cortés-Ortuño, W. Wang, O. Hovorka, C. H. Marrows, and H. Fangohr, Skyrmions in thin films with easy-plane magnetocrystalline anisotropy, *Appl. Phys. Lett.* 108(13), 132406 (2016)

23. S. Huang and C. Chien, Extended skyrmion phase in epitaxial FeGe (111) thin films, *Phys. Rev. Lett.* 108(26), 267201 (2012)

24. Y. Li, N. Kanazawa, X. Z. Yu, A. Tsukazaki, M. Kawasaki, M. Ichikawa, X. F. Jin, F. Kagawa, and Y. Tokura, Robust formation of skyrmions and topological Hall effect anomaly in epitaxial thin films of MnSi, *Phys. Rev. Lett.* 110(11), 117202 (2013)

25. P. Bruno, V. Dugaev, and M. Taillefumier, Topological Hall effect and Berry phase in magnetic nanostructures, *Phys. Rev. Lett.* 93(9), 096806 (2004)

26. Y. Tokunaga, X. Z. Yu, J. S. White, H. M. Rønnow, D. Morikawa, Y. Taguchi, and Y. Tokura, A new class of chiral materials hosting magnetic skyrmions beyond room temperature, *Nat. Commun.* 6(1), 7638 (2015)

27. J. Rowland, S. Banerjee, and M. Randeria, Skyrmions in chiral magnets with Rashba and Dresselhaus spin–orbit coupling, *Phys. Rev. B* 93(2), 020404 (2016)

28. S. Rohart and A. Thiaville, Skyrmion confinement in ultrathin film nanostructures in the presence of Dzyaloshinskii–Moriya interaction, *Phys. Rev. B* 88(18), 184422 (2013)

29. B. Bian, G. Chen, Q. Zheng, J. Du, H. Lu, J. P. Liu, Y. Hu, and Z. Zhang, Self-assembly of CoPt magnetic nanoparticle arrays and its underlying forces, *Small* 14(34), 1801184 (2018)

30. W. Jiang, P. Upadhyaya, W. Zhang, G. Yu, M. B. Jungfleisch, F. Y. Fradin, J. E. Pearson, Y. Tserkovnyak, K. L. Wang, O. Heinonen, S. G. E. te Velthuis, and A. Hoffmann, Blowing magnetic skyrmion bubbles, *Science* 349(6245), 283 (2015)

31. B. Heim, T. F. Rønnow, S. V. Isakov, and M. Troyer, Quantum versus classical annealing of Ising spin glasses, *Science* 348(6231), 215 (2015)

32. R. Li, L. Yu, and Y. Hu, Spin-glass irreversibility temperature and magnetic stabilization in ferromagnet/spin-glass bilayers, *Phys. Status Solidi Rapid Res. Lett.* 13(6), 1900039 (2019)

33. X. Chi, R. Li, L. Yu, H. Kou, A. Du, Y. Liu, and Y. Hu, Spin glass properties mapped by coercivity in ferromagnet/spin glass bilayers, *Nanotechnology* 30(12), 125702 (2019)

34. X. D. Chi and Y. Hu, Modulation of skyrmion diameter in centrosymmetric frustrated magnet, *Acta Physica Sinica* 67, 137502 (2018)

35. N. Romming, A. Kubetzka, C. Hanneken, K. von Bergmann, and R. Wiesendanger, Field-dependent size and shape of single magnetic skyrmions, *Phys. Rev. Lett.* 114(17), 177203 (2015)

36. S. von Malottki, B. Dupé, P. F. Bessarab, A. Delin, and S. Heinze, Enhanced skyrmion stability due to exchange frustration, *Sci. Rep.* 7(1), 12299 (2017)

37. N. C. Koon, Calculations of exchange bias in thin films with ferromagnetic/antiferromagnetic interfaces, *Phys. Rev. Lett.* 78(25), 4865 (1997)

38. H. Du, W. Ning, M. Tian, and Y. Zhang, Field-driven evolution of chiral spin textures in a thin helimagnet nanodisk, *Phys. Rev. B* 87(1), 014401 (2013)

39. H. Du, R. Che, L. Kong, X. Zhao, C. Jin, C. Wang, J. Yang, W. Ning, R. Li, C. Jin, X. Chen, J. Zang, Y. Zhang, and M. Tian, Edge-mediated skyrmion chain and its collective dynamics in a confined geometry, *Nat. Commun.* 6(1), 8504 (2015)

40. X. Z. Yu, N. Kanazawa, Y. Onose, K. Kimoto, W. Z. Zhang, S. Ishiwata, Y. Matsui, and Y. Tokura, Near room-temperature formation of a skyrmion crystal in thin-films of the helimagnet FeGe, *Nat. Mater.* 10(2), 106 (2011)